

# Fractional flux quanta at intrinsic metallic interfaces of noncentrosymmetric superconductors

C. Iniotakis,<sup>1</sup> S. Fujimoto,<sup>2</sup> and M. Sigrist<sup>1</sup>

<sup>1</sup>*Institute for Theoretical Physics, ETH Zurich, 8093 Zurich, Switzerland*

<sup>2</sup>*Department of Physics, Kyoto University, Kyoto 606-8502, Japan*

(Dated: May 6, 2019)

We examine intrinsic interfaces separating crystalline twin domains of opposite spin-orbit coupling in a noncentrosymmetric superconductor such as CePt<sub>3</sub>Si. At these interfaces, low-energy Andreev bound states occur as a consequence of parity-mixed Cooper pairing, and a superconducting phase which violates time reversal symmetry can be realized. This provides an environment allowing flux lines with fractional flux quanta to be formed at the interface. Their presence could have strong implications on the flux creep behavior in such superconductors.

PACS numbers: 74.20.Rp, 74.50.+r, 74.70.Tx

Symmetry is a decisive factor for many properties of materials. Lowering a symmetry can yield new couplings between physical observables and causes intriguing phenomena. The recently discovered noncentrosymmetric superconductors CePt<sub>3</sub>Si, CeRhSi<sub>3</sub>, CeIrSi<sub>3</sub>, and Li<sub>2</sub>(Pt<sub>x</sub>Pd<sub>1-x</sub>)<sub>3</sub>B provide such examples [1, 2, 3, 4]. In these materials, the absence of an inversion center generates antisymmetric spin-orbit interaction and leads, in the superconducting state, to parity-mixing of Cooper pairs, magnetoelectric effects, and many other interesting features [5, 6, 7, 8]. In many cases, such crystal structures permit the existence of twin domains exhibiting opposite inversion symmetry breaking within a single crystal. Actually, in the crystal growth processes of noncentrosymmetric materials, the formation of such twin domains is inevitable. The existence of twin domains in noncentrosymmetric superconductors is also suggested by a recent experiment, which revealed that a high quality single crystal sample of CePt<sub>3</sub>Si exhibits a lower transition temperature than polycrystal ones [9]. Since the origin of this behavior cannot be understood in terms of conventional impurity effects [10], possibly twin boundaries could enhance the trend to superconductivity. Furthermore, recent NMR measurements of the single crystal sample are ingeniously interpreted by assuming the existence of twin domains [11]. Motivated by these observations, in this letter, we investigate effects of intrinsic interfaces between twin domains on the parity-mixed superconducting state. Our central finding is, that superconducting states with broken time-reversal symmetry can occur at the interfaces, allowing for fractional vortices.

We consider a noncentrosymmetric superconductor such as CePt<sub>3</sub>Si and assume for simplicity a spherical Fermi surface parametrized by the unit vector  $\hat{\mathbf{k}} = (\cos \varphi \sin \theta, \sin \varphi \sin \theta, \cos \theta)$ . The presence of a Rashba-type spin-orbit coupling,  $\alpha(\hat{\mathbf{z}} \times \hat{\mathbf{k}}) \cdot \mathbf{s}$ , induces a splitting of the electron bands and the Fermi surface into sheets, each exhibiting a specific spin structure. The superconducting

phase displays a mixed parity [5, 6, 7], and the state compatible with experiments consists of an  $s$ - and a  $p$ -wave component, being of  $s \pm p$ -character on the two Fermi sheets. Moreover, there is experimental evidence for a nodal gap structure, which suggests a dominant spin-triplet  $p$ -wave component with  $q = \Delta_s/\Delta_p < 1$ , where  $\Delta_s$  and  $\Delta_p$  denote the magnitudes of the  $s$ - and the  $p$ -wave components in the superconducting gap [12, 13]. For the calculations, we employ quasiclassical Eilenberger theory of superconductivity [14, 15, 16]. This method provides a convenient and powerful tool for describing superconductivity and has been applied to noncentrosymmetric superconductors in Ref. [13]. According to Ref. [17], the superconducting state can be expressed by the so-called bulk coherence functions  $\gamma_B, \tilde{\gamma}_B$  straightforwardly, which corresponds to the Riccati formulation of Eilenberger theory [18, 19]. Using an effective one-band description, where the size of the band splitting is assumed to be small compared to the Fermi energy, we obtain [17]

$$\gamma_B = -(\gamma_+ \hat{\sigma}_+ + \gamma_- \hat{\sigma}_-) \hat{\sigma}_y \quad (1a)$$

$$\tilde{\gamma}_B = \hat{\sigma}_y (\gamma_+ \hat{\sigma}_+ + \gamma_- \hat{\sigma}_-), \quad (1b)$$

where the coefficients are defined as

$$\gamma_{\pm} = \frac{\Delta_{\pm}}{\omega_n + \sqrt{\omega_n^2 + |\Delta_{\pm}|^2}} \quad (2)$$

with  $\Delta_{\pm}(\hat{\mathbf{k}}) = \Delta_s \pm \Delta_p \sin \theta$  and  $\omega_n = (2n + 1)\pi k_B T$  denoting Matsubara frequencies. While we neglect the splitting of the bands, we keep their spin structure imposed by the spin-orbit coupling, as described by

$$\hat{\sigma}_{\pm} = \frac{1}{2} \begin{pmatrix} 1 & \mp i e^{-i\varphi} \\ \pm i e^{i\varphi} & 1 \end{pmatrix}. \quad (3)$$

These spin matrices have the useful projection properties  $\hat{\sigma}_{\pm}^2 = \hat{\sigma}_{\pm}$ ,  $\hat{\sigma}_+ \hat{\sigma}_- = \hat{\sigma}_- \hat{\sigma}_+ = 0$  and  $\hat{\sigma}_+ + \hat{\sigma}_- = 1$ .

We now turn to the electronic properties of an interface separating regions  $A$  and  $B$ , which are characterized

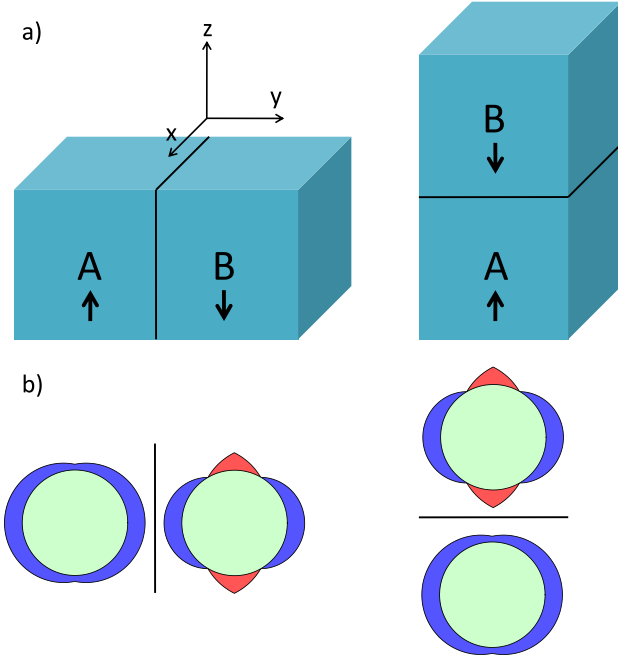


FIG. 1: Sketch of two intrinsic metallic interfaces in a noncentrosymmetric superconductor with normal vector  $\hat{\mathbf{n}}$  perpendicular (left) or parallel (right) to the  $z$ -axis. a) The interface separates regions  $A$  and  $B$ , which exhibit a different direction of the spin-orbit coupling  $\alpha$  as indicated by the arrows. b) The situation is analogous to a junction between two ordinary singlet superconductors with gap amplitudes  $\Delta_+$  and  $-\Delta_-$ . The sign of the gap amplitude is illustrated by the two different colors.

by the opposite sign of the antisymmetric spin orbit coupling according to  $\alpha_A = -\alpha_B$ . An illustration of two specific situations for such an interface can be found in Fig. 1, a), and similar setups have already been examined in a different context [20, 21]. For our following analysis we neglect the direct influence of the interface on the superconducting order parameter and fix the moduli of the pair potentials to remain constant even at the interface. This approximation does not affect our discussion qualitatively, and quantitative corrections are minor. It leads to the simplification, however, that the coherence functions at the interface can be replaced by the corresponding bulk coherence functions. In the following, we use bulk coherence functions  $\gamma^A$  and  $\tilde{\gamma}^A$  for region  $A$  according to Eqs. (1). Regarding region  $B$ , one might be tempted to get the bulk coherence functions  $\gamma^B$  and  $\tilde{\gamma}^B$  by simply interchanging the two gap amplitudes  $\Delta_{\pm}$ . For small values of  $q$  it is rather natural, however, to keep the dominant  $p$ -wave component  $\Delta_p$  constant on both sides of the interface. Then, the  $s$ -wave component changes its sign across the interface and an additional phase factor  $-1$  has to be introduced on side  $B$ . We allow the gap function of region  $B$  to exhibit a further general phase difference with respect to region  $A$ , which is denoted by  $\phi$  in the following. The bulk coherence functions of region

$B$  are then given by

$$\gamma^B = (\gamma_- \hat{\sigma}_+ + \gamma_+ \hat{\sigma}_-) \hat{\sigma}_y e^{i\phi} \quad (4a)$$

$$\tilde{\gamma}^B = -\hat{\sigma}_y (\gamma_- \hat{\sigma}_+ + \gamma_+ \hat{\sigma}_-) e^{-i\phi}. \quad (4b)$$

Generally, once the coherence functions  $\gamma, \tilde{\gamma}$  are known for a specific Fermi vector at a given point in space, also the quasiclassical Green's function  $\hat{g}$  in  $2 \times 2$  spin space is immediately available as

$$\hat{g} = (1 - \gamma \tilde{\gamma})^{-1} (1 + \gamma \tilde{\gamma}) = 2(1 - \gamma \tilde{\gamma})^{-1} - 1. \quad (5)$$

The interface is implemented by well-established boundary conditions for the Green's function or the coherence functions, respectively [19, 22, 23]. Restricting ourselves to a high-transparency interface, the resulting Green's function directly at the interface is given by

$$\begin{aligned} \hat{g} &= 2(1 - \gamma^A \tilde{\gamma}^B)^{-1} - 1 \\ &= 2[1 - (\gamma_+ \hat{\sigma}_+ + \gamma_- \hat{\sigma}_-) (\gamma_- \hat{\sigma}_+ + \gamma_+ \hat{\sigma}_-) e^{-i\phi}]^{-1} - 1 \\ &= 2[1 - (\gamma_+ \gamma_- \hat{\sigma}_+ + \gamma_- \gamma_+ \hat{\sigma}_-) e^{-i\phi}]^{-1} - 1 \\ &= \frac{2}{1 - \gamma_+ \gamma_- e^{-i\phi}} - 1, \end{aligned} \quad (6)$$

where the projection properties of  $\hat{\sigma}_{\pm}$  have been used in the intermediate steps. Note, that the expression Eq. (6) for the quasiclassical Green's function at the interface only holds for quasiparticle trajectories with Fermi vectors  $\hat{\mathbf{k}}$  pointing from  $A$  to  $B$ . In the opposite case, the superscripts  $A$  and  $B$  have to be interchanged, and we find the symmetry relation  $\hat{g}(\omega_n, -\hat{\mathbf{k}}) = \hat{g}(\omega_n, \hat{\mathbf{k}})^*$ . Several points should be mentioned here. Firstly, only bands having the same spin structure,  $\hat{\sigma}_+$  or  $\hat{\sigma}_-$ , contribute to this Green's function, the other combinations vanish by projection. Furthermore, the Green's function is proportional to the unit matrix. As a consequence, there is an analogy between this interface of noncentrosymmetric superconductors and a standard interface consisting of two singlet superconductors as illustrated in Fig. 1, b).

In the following, we derive the Josephson current density through the interface. Using the symmetry relation stated above, we find

$$\mathbf{j}(\phi) = 4\pi e N_0 k_B T v_F \sum_{\omega_n > 0}^{\omega_c} \langle \hat{\mathbf{k}} \text{Im}[g] \rangle, \quad (7)$$

where  $\langle \dots \rangle$  denotes averaging over half of the Fermi sphere determined by quasiparticle directions  $\hat{\mathbf{k}}$  pointing from region  $A$  to  $B$ , and  $g$  is the unit matrix component of  $\hat{g}$  according to Eq. (6). Written in normalized quantities  $\hat{T} = T/T_c$  and  $\hat{j} = j/4\pi e N_0 k_B T_c v_F$ , we eventually find the result

$$\hat{\mathbf{j}}(\phi) = \hat{T} \sum_{\omega_n > 0}^{\omega_c} \int_0^{\frac{\pi}{2}} d\theta \left\{ \frac{\frac{4}{\pi} \sin^2 \theta}{\sin 2\theta} \right\} \text{Im} \left[ \frac{1}{1 - \gamma_+ \gamma_- e^{-i\phi}} \right] \hat{\mathbf{n}}, \quad (8)$$

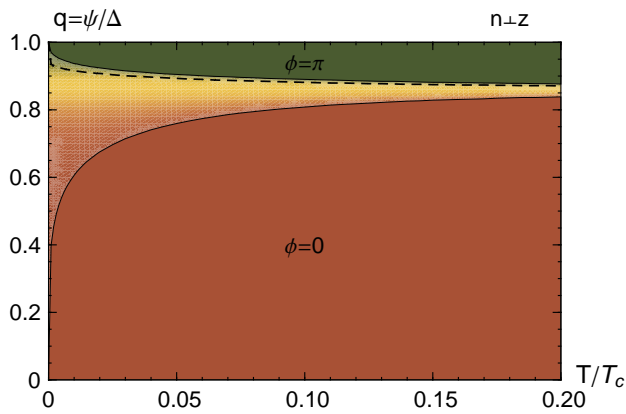


FIG. 2: (Color online) Part of the  $q, T$ -phase diagram of an intrinsic metallic junction in a noncentrosymmetric superconductor. There are regions of a stable Josephson phase  $\phi = 0$  (bottom) and  $\phi = \pi$  (top). In between, a phase difference  $0 < \phi < \pi$  is favorable. Here, the normal vector  $\hat{\mathbf{n}}$  of the interface is taken to be perpendicular to the  $z$  axis, corresponding to the lefthand scenario of Fig. 1. For  $T \rightarrow T_c$ , 0- and  $\pi$ -phase meet at  $q = \sqrt{3}/2 \approx 0.87$ . The dashed line indicates the boundary between 0- and  $\pi$ -phase in the contrary scenario of a low-transparency tunnel junction.

where the upper (lower) formula stands for the situation with the normal vector  $\hat{\mathbf{n}}$  of the interface perpendicular (parallel) to the  $z$ -axis of the system. In both cases only components of the current flowing perpendicular to the interface are allowed by symmetry. The values of  $\gamma_+, \gamma_-$  in the integrand are real and depend on  $\sin \theta$  themselves [cf. Eq. (2)].

Numerical evaluation of the current-phase relations according to Eq. (8) allows us to determine the phase difference  $\phi$  of the stable interface states. We focus on  $\phi > 0$ , keeping in mind that with  $\phi$  also  $-\phi$  is a stable solution. For the two situations depicted in Fig. 1 we can derive the phase diagrams displayed in Figs. 2 and 3, respectively. We find three regions in the  $q$ - $T$ -phase diagram. In the region of small  $q$ , the stable state corresponds to  $\phi = 0$  and for  $q$  close to one it is  $\phi = \pi$ . The latter means, that the  $s$ -wave component  $\Delta_s$  would remain unchanged across the interface. Intriguing is a region in between these two limits, where the stable phase difference has an intermediate value  $0 < \phi < \pi$ . Note, that the  $\pm\phi$  solutions are degenerate for this intermediate region, reflecting the fact that such an interface state is time-reversal symmetry breaking, since  $\phi$  changes sign under the time reversal operation. The intermediate region of  $q$ -values shrinks with increasing temperature, eventually reaching a single point at  $T_c$ . For the normal vector perpendicular (parallel) to  $z$  this value is  $q = \sqrt{3}/2 \approx 0.87$  ( $q = 1/\sqrt{2} \approx 0.71$ ) within our model.

Qualitatively, the phase diagram can be understood as a consequence of Andreev bound states occurring at the interface. A sign-change of the gap function along

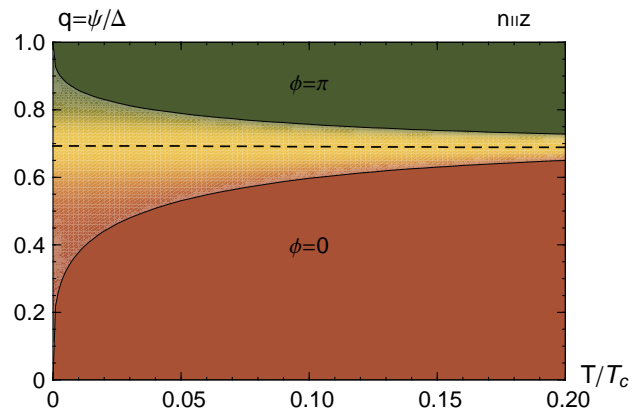


FIG. 3: (Color online) Part of the  $q, T$ -phase diagram of an intrinsic metallic junction in a noncentrosymmetric superconductor. There are regions of a stable Josephson phase  $\phi = 0$  (bottom) and  $\phi = \pi$  (top). In between, a phase difference  $0 < \phi < \pi$  is favorable. Here, the normal vector  $\hat{\mathbf{n}}$  of the interface is taken to be parallel to the  $z$  axis, corresponding to the righthand scenario of Fig. 1. For  $T \rightarrow T_c$ , 0- and  $\pi$ -phase meet at  $q = 1/\sqrt{2} \approx 0.71$ . The dashed line indicates the boundary between 0- and  $\pi$ -phase in the contrary scenario of a low-transparency tunnel junction.

a quasiparticle trajectory gives rise to the formation of zero-energy Andreev bound states. Such sign changes occur as soon as  $q > 0$ . Changing the phase difference  $\phi$  from zero to a finite value may move these bound states away from zero energy, resulting in an energy gain accordingly. For larger values of  $q$  the original spectral weight of the zero-energy Andreev bound states gets enhanced. Consequently, upon increasing  $q$  a continuous transition to a state of finite  $\phi$  occurs at some critical value  $q_c(T)$ . If  $q$  is increased further,  $\phi$  eventually reaches the upper limiting value  $\pi$ .

The extent of the intermediate region in the phase diagram depends on the transparency of the intrinsic interface. The results presented so far have been derived under the assumption of a high-transparency metallic junction. For comparison, we also examined the Josephson current for the opposite limit of a low-transparency tunnel junction. Employing standard boundary conditions for the quasiclassical propagators [19, 22, 23], we find

$$\hat{\mathbf{j}}(\phi) = D \sin \phi \cdot \hat{T} \sum_{\omega_n > 0}^{\omega_c} \int_0^{\frac{\pi}{2}} d\theta \left\{ \frac{4}{\pi} \frac{\sin^2 \theta}{\sin 2\theta} \frac{c_{\perp}}{c_{\parallel}} \right\} \hat{\mathbf{n}}, \quad (9)$$

where the following notation is used

$$c_{\perp} = \frac{-\gamma_- \gamma_+}{(1 + \gamma_- \gamma_+)(\gamma_- - \gamma_+)} \arctan \frac{\gamma_- - \gamma_+}{1 + \gamma_- \gamma_+} \quad (10a)$$

$$c_{\parallel} = \frac{-\gamma_- \gamma_+}{(1 + \gamma_-^2)(1 + \gamma_+^2)}. \quad (10b)$$

These results are valid to first order in the transparency  $D \ll 1$ , and, as in Eq. (8) for the metallic interface, the

upper formula corresponds to the orientation  $\hat{\mathbf{n}} \perp \hat{\mathbf{z}}$  and the lower one to  $\hat{\mathbf{n}} \parallel \hat{\mathbf{z}}$ . The main difference to the metallic case can be seen quite clearly: Since the current-phase relation in Eq. (9) is purely sinusoidal, the stable phase of the junction must be either 0 or  $\pi$ , depending on the sign of the amplitude factor. In particular, the intermediate region has been shrunk to a single boundary line in the phase diagram. In Figs. 2 and 3, these boundaries between 0- and  $\pi$ -regions in the tunnel limit are sketched by the dashed lines for comparison.

In the following, we concentrate on one remarkable physical consequence of the intermediate region where  $\phi \neq 0, \pi$ . The degeneracy of the two phases  $\pm\phi$  gives rise to the possibility of line defects on the interface which carry fractional magnetic flux. They can exist at the interface only, and may generally exhibit fractional flux quanta  $\Phi$  according to

$$\frac{\Phi}{\Phi_0} = n \pm \frac{\phi}{\pi} \quad n \in \mathbb{Z}, \quad (11)$$

where  $\Phi_0 = hc/2e$  is the standard flux quantum. As a consequence of this property, it is possible for a standard vortex to decay into two fractional ones on the interface, carrying the fractional flux  $\phi/\pi \cdot \Phi_0$  and  $(1 - \phi/\pi) \cdot \Phi_0$ , respectively. Both of these line defects are strongly pinned to the interface. If there are many of these fractional vortices lined up along the interface, they can act as a severe impediment for flux flow. Similar theoretical considerations have been made for domain walls in time reversal symmetry breaking superconductors [24, 25, 26].

In summary, we find that interfaces between twin domains in a noncentrosymmetric superconductor such as CePt<sub>3</sub>Si could possess unusual properties. They can host low-energy Andreev bound states and, under certain conditions, give rise to a time reversal symmetry violating phase, a characteristic phase of the interface only. In this situation, fractional vortices could exist on the interface and severely influence the flux creep. Since the interface properties are different for different orientations, the flux creep properties would likely depend on the vortex direction. Furthermore, the change of the phase  $\phi$  across such an interface can also modify special interference features of the Josephson effect in a magnetic field, if the interface intersects the junction between a noncentrosymmetric and a conventional superconductor. The low-energy Andreev bound states may be directly accessible by local tunneling probes such as scanning tunneling microscopes.

We would like to thank D.F. Agterberg, N. Hayashi, Y. Kitaoka, H. Mukuda and Y. Onuki for stimulating

discussions. This work was financially supported by the Swiss Nationalfonds and the NCCR MaNEP, as well as the Center for Theoretical Studies of ETH Zurich.

- 
- [1] E. Bauer, G. Hilscher, H. Michor, Ch. Paul, E.W. Scheidt, A. Griбанov, Yu. Seropegin, H. Noël, M. Sigrist, and P. Rogl, Phys. Rev. Lett. **92**, 027003 (2004).
  - [2] N. Kimura, K. Ito, K. Saitoh, Y. Umeda, H. Aoki, and T. Terashima, Phys. Rev. Lett. **95**, 0247004 (2005).
  - [3] I. Sugitani, Y. Okuda, H. Shishido, T. Yamada, A. Thamizhavel, E. Yamamoto, T.D. Matsuda, Y. Haga, T. Takeuchi, R. Settai, and Y. Onuki, J. Phys. Soc. Jpn. **75**, 043703 (2006).
  - [4] K. Togano, P. Badica, Y. Nakamori, S. Orimo, H. Takeya, and K. Hirata, Phys. Rev. Lett. **93**, 247004 (2004).
  - [5] V.M. Edelstein, Sov. Phys. JETP **68**, 1244 (1989).
  - [6] L.P. Gor'kov and E.I. Rashba, Phys. Rev. Lett. **87**, 037004 (2001).
  - [7] P.A. Frigeri, D.F. Agterberg, A. Koga, and M. Sigrist, Phys. Rev. Lett. **92**, 097001 (2004).
  - [8] S. Fujimoto, Phys. Rev. B **72**, 024515 (2005).
  - [9] T. Takeuchi, T. Yasuda, M. Tsujino, H. Shishido, R. Settai, H. Harima, and Y. Onuki, J. Phys. Soc. Jpn. **76**, 014702 (2007).
  - [10] V.P. Mineev and K.V. Samokhin, Phys. Rev. B **75**, 184529 (2007).
  - [11] H. Mukuda, S. Nishida, A. Harada, M. Yashima, Y. Kitaoka, M. Tsujino, R. Settai, and Y. Onuki, unpublished.
  - [12] I. Bonalde, W. Brämer-Escamilla, and E. Bauer, Phys. Rev. Lett. **94**, 207002 (2005).
  - [13] N. Hayashi, K. Wakabayashi, P.A. Frigeri, and M. Sigrist, Phys. Rev. B **73**, 024504 (2006).
  - [14] G. Eilenberger, Z. Phys. **214**, 195 (1968).
  - [15] A.I. Larkin and Yu.N. Ovchinnikov, Zh. Éksp. Teor. Fiz. **55**, 2262 (1968); Sov. Phys. JETP **28**, 1200 (1969).
  - [16] J.W. Serene and D. Rainer, Phys. Rep. **101**, 221 (1983).
  - [17] C. Iniotakis, N. Hayashi, Y. Sawa, T. Yokoyama, U. May, Y. Tanaka, and M. Sigrist, Phys. Rev. B **76**, 012501 (2007).
  - [18] N. Schopohl and K. Maki, Phys. Rev. B **52**, 490 (1995); N. Schopohl, cond-mat/9804064 (1998).
  - [19] M. Eschrig, Phys. Rev. B **61**, 9061 (2000).
  - [20] K. Børkje and A. Sudbø, Phys. Rev. B **74**, 054506 (2006).
  - [21] K. Børkje, Phys. Rev. B **76**, 184513 (2007).
  - [22] A.V. Zaitsev, Zh. Éksp. Teor. Fiz. **86**, 1742 (1984); Sov. Phys. JETP **59**, 1015 (1984).
  - [23] A. Shelankov and M. Ozana, Phys. Rev. B **61**, 7077 (2000).
  - [24] G.E. Volovik and L.P. Gor'kov, Pis'ma Zh. Éksp. Teor. Fiz. **39**, 550 (1984); JETP Lett. **39**, 674 (1984).
  - [25] M. Sigrist and K. Ueda, Rev. Mod. Phys. **63**, 239 (1991).
  - [26] M. Sigrist and D.F. Agterberg, Progr. Theor. Phys. **102**, 965 (1999).